Dynamic Range Requirements for Microcellular Personal Communication Systems Using Analog Fiber-Optic Links

J. C. Fan, C. L. Lu, and L. G. Kazovsky, *Fellow, IEEE*

***Abstract*— Fiber infrastructures in future personal communication systems (PCS's) must minimize remote antenna size and cost, and facilitate system maintenance and upgradeability. These goals can be met by a centralized PCS infrastructure using analog fiber-optic links. It is essential that the relationship between optical-link quality in terms of spurious-free dynamic range (SFDR) and PCS quality of service be accurately quantified so that optical device and other infrastructure design requirements can be determined. This paper presents a comprehensive wireless/optical simulation model which combines wireless system characteristics (such as fading, cochannel interference, diversity, and power control) with the noise and nonlinearities of fiber-optic links. Results of the simulation indicate that representative SFDR requirements for fiber infrastructures in PCS systems are in the 72–83 dB $\cdot$ Hz$^{2/3}$ range. The impact of varying environmental characteristics as quantified by distance loss and shadowing variance is between 7–10 dB. A larger distance loss or lower shadowing variance result in lower SFDR requirements. The required automatic gain control (AGC) accuracy decreases as the SFDR increases. These results indicate that either distributed feedback (DFB) or Fabry–Perot (FP) semiconductor laser diodes can be used in the implementation of PCS infrastructures.**

***Index Terms*—Analog fiber, dynamic range, fading, infrastructure, laser, PCS, power control, SFDR, wireless.**

I. Introduction

THE goals of microcellular personal communication systems (PCS's) include service availability over an extremely high percentage of user environments, and provision of a combination of services such as voice, data, fax, and video. To provide such enhanced services with high quality of service, PCS providers must use a remote antenna density of tens, hundreds, or even thousands of antennas per square kilometer. This antenna density enables the accommodation of more subscribers per unit service area and the use of smaller and lower power handsets.

To reduce the cost of PCS deployment, it is essential that each microcell be served by a compact, relatively inexpensive remote antenna. A large number of these remote antennas can then be connected via optical fiber to a single base station at an economical location. We refer to this type of fiber infrastructure as a centralized processing infrastructure. An infrastructure of this type has been widely proposed as a viable PCS backbone [1]–[3]. This infrastructure is discussed in Section V of this paper.

There are a variety of advantages to centralized processing. Some of these include [3], [4]: 1) simplicity: there is no need for RF frequency conversion or receiver hardware at the remote antenna; 2) potential hardware savings at the base station: since busy hours for downtown and residential areas served by a base station may be quite different, only enough receiver hardware to handle the busiest hour across the entire base-station coverage area is required at the base station, instead of the full complement of receiver hardware at each remote antenna; 3) repairs and service upgrades at a centralized location are most convenient and cost effective; and 4) dynamic RF carrier allocation can potentially be implemented from a centralized location.

The primary disadvantage of this infrastructure is that the signal traverses the fiber in analog form. Since detection of the desired voice/data is not performed until the RF signal is received at the base station, the noise and nonlinearities generated by the optical transmitter and receiver will combine with interference and multipath from the wireless environment to degrade PCS quality of service. The severity of this performance degradation determines the performance requirements which must be met by the optical devices used in the infrastructure.

The goal of this paper is to accurately quantify the relationship between optical-link quality, as quantified by spurious-free dynamic range (SFDR), and PCS quality of service. To achieve this goal, a comprehensive wireless/optical model has been developed which combines the simulated performance of Bellcore's Wireless/Personal Access Communication System (WACS/PACS) with the noise and nonlinearities of fiber-optic links. This paper extends previous literature [1]–[3] by taking into account the impact of characteristics of the wireless system and environment. These characteristics include fading, shadowing, selection diversity, and power control.

This paper is organized as follows. Section II contains a brief background on the SFDR of analog fiber-optic links. Section III contains a brief background on the WACS/PACS system. Section IV presents the PCS simulation model. Section V describes the interaction of the PCS air interface (or wireless link layer) and analog fiber-optic links, and explains how the imperfections of analog links will impact PCS quality of service. Section VI presents results showing the impact of optical-link SFDR on PCS performance in terms of aerial

Manuscript received December 6, 1996; revised May 12, 1997.

The authors are with Globalstar, L. P., San Jose, CA 95164 USA, and also with the Department of Electrical Engineering, Stanford University, Stanford, CA 94305 USA.

Publisher Item Identifier S 0018-9480(97)06008-0.

TABLE I
CHARACTERISTICS OF THE WACS/PACS PCS SYSTEM [7]

	WACS/PACS		WACS/PACS
System Type	PCS, microcell (100-500 meter radius)	**Number of RF Carriers per Cell**	1
Coverage Availability	98-100%	**Voice Channels per RF Carrier**	8
Frequency Band	Two 5 or 10 MHz blocks within 1850-1990 MHz	**Total RF Carriers Used**	8 or 16 pairs, 300 kHz spacing
Access Format	FDMA/TDMA	**Bit Rate per Carrier**	384 kbit/s
Modulation	$\pi/4$ DQPSK	**Bandwidth per Carrier**	270 kHz
SIR Requirement	11 dB	**Voice Bit Rate per User**	32 kbit/s
Reuse Factor	8 or 16	**Power Control Range**	30 dB, 0.75 dB steps
Propagation Parameters	Distance loss exponent = 4 - 6; Shadowing std. deviation = 8 - 14 dB	**Channel Compensation**	Diversity

availability for a variety of wireless environments. Section VII presents a discussion. Section VIII presents conclusions.

II. SFDR OF ANALOG FIBER-OPTIC LINKS

The SFDR of an analog optical link is the range of RF input powers for which a two-tone RF input signal can be clearly distinguished from noise and nonlinearities at the link output. The minimum RF input power in this range is that which results in the received signal just reaching the noise floor generated by receiver noise and laser relative intensity noise (RIN). The maximum RF input power is that at which the in-band third-order intermodulation power generated by laser or external modulator nonlinearities just reaches the noise floor.

The SFDR for a direct-detection analog optical link is derived in detail in [5], [6]. From [5], [6], the SFDR of an externally modulated direct detection analog link can be found as

$$\mathrm{SFDR} = \left[\frac{8}{3|b_3|}\frac{R^2P_{\mathrm{opt}}^2}{2\left(2qRP_{\mathrm{opt}} + \frac{4kT}{R_r} + R^2P^2 10^{\frac{\mathrm{RIN}}{10}}\right)B}\right]^{2/3} = \left[\frac{8}{3|b_3|}\mathrm{SNR}_0\right]^{2/3} \quad (1)$$

where R is the photodiode responsivity, P_{opt} is the average received optical power, b_3 is the third-order nonlinearity coefficient, B is the bandwidth at the receiver output, and SNR_0 is the normalized SNR for unity modulation depth. The three terms in parentheses in the denominator are the power spectral densities (PSD's) of the shot, thermal, and RIN's, respectively. In those terms, q is the charge of an electron, R is the photodiode responsivity, R_r is the receiver equivalent front-end resistance, and RIN (in decibel/hertz) is the measured strength of the intensity noise relative to the optical carrier. The optimum optical modulation depth corresponding to this SFDR is the modulation depth at which the third-order intermodulation distortion power (IMP) equals the noise power. This can be thought of as the modulation depth which balances the impact of noise and IMP's. The optimum modulation depth is given by [5], [6]

$$m_{\mathrm{opt}} = \left[\frac{64}{9b_3^2\mathrm{SNR}_0}\right]^{1/6}. \quad (2)$$

Similar expressions can be derived for directly modulated analog optical links.

III. CHARACTERISTICS OF WACS/PACS

The Bellcore WACS/PACS standard [7] is designed for future low-tier PCS systems serving primarily hand-held phone users. Table I contains key characteristics of the WACS/PACS standard which are used in the comprehensive simulation model in this paper.

Table I refers to 98%–100% coverage availability for WACS/PACS. Aerial availability refers to the percentage of randomly selected locations at which a user can attain adequate link quality at any given time as measured by signal-to-interference ratio (SIR). Availability is purely a measure of system coverage at any instant, and does not quantify the likelihood of any individual call lasting for a specified duration. This is because the likelihood of any individual call lasting for a specified duration depends on user behavior, for which no accurate models are available in the literature, as well as on the physical characteristics of the environment.

Exactly one RF carrier is allocated to each WACS/PACS microcell. Up to eight voice conversations at 32 kb/s can be time-division multiplexed on each RF carrier. The overall bit rate of 384 kb/s includes overhead bits associated with each time slot. The bandwidth of 270 kHz per carrier corresponds to the 0.7-bandwidth bit-time product for quadrature phase-shift keying (QPSK) [8]. The SIR required for adequate received-signal quality is 11 dB [7], [9]. The reuse factor used in

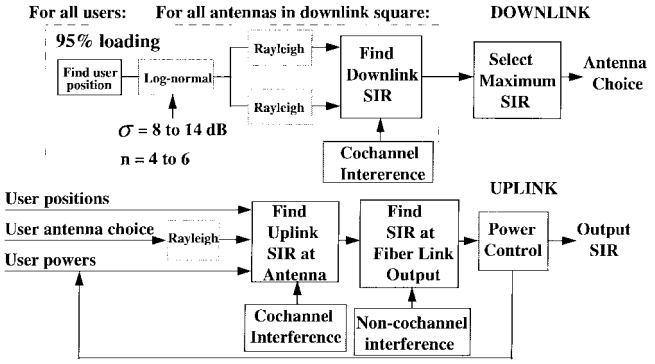

Fig. 1. Block diagram of simulation procedure.

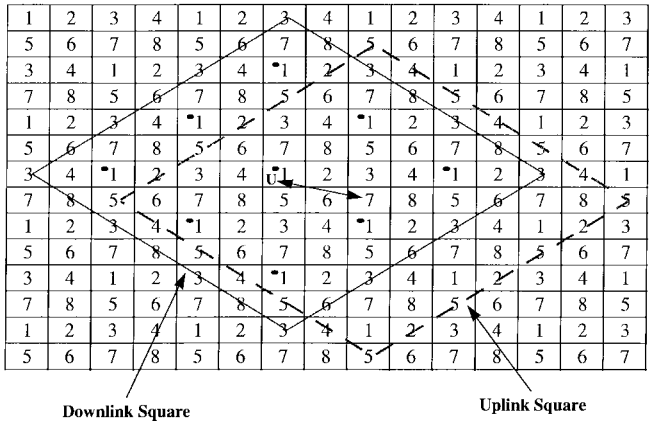

Fig. 2. Frequency reuse pattern with squares used for downlink (solid) and uplink (dashed) computations marked.

this paper (and elsewhere in the literature) is 8 [7], [9]; it is desirable for the reuse factor to be as small as possible to reduce overall system bandwidth requirements. The power control range is 30 dB with 0.75 dB steps. The 400-Hz power control speed is easily able to react to the terrain-dependent log-normal fading and multipath fading seen by hand-held users, which is at fastest in the tens of hertz [5]. The chosen means for WACS/PACS to compensate for multipath fading effects is selection diversity, which refers to the use of two antennas within a remote antenna or a user phone to create uncorrelated multipath fading channels. At any given time, the fading channel which gives the higher SIR at the receiver is selected.

The range of propagation-loss exponents in this system ranges from 4 (for free-space propagation plus a single reflected path) to 6. The range of shadowing standard deviations is from 8 to 14 dB. Both of these have been determined through best fits to measured data from urban and suburban outdoor environments in the literature [10]–[12]. (Indoor environments follow a characteristic better approximated by $\exp(-kd)$, with d being distance [7]. These environments are difficult to model outside of specific case studies.)

IV. PCS Simulation Model

In this section, the PCS simulation model is described in detail.

The overall simulation block diagram is shown in Fig. 1. Users are randomly placed onto a 52×52 grid until the system is loaded to 95% capacity over all frequencies and time slots to simulate the worst-case performance of the system.

To minimize edge effects, aerial availability statistics are computed only over the central 24×24 grid. These statistics are averaged over the eight time slots (that are uncorrelated) and over multiple runs (usually around ten runs) to ensure that the error bars of the availability statistics are small relative to the variations measured in the results presented in Section VI.

A. Frequency Reuse Pattern and Macrodiversity

The eight-frequency reuse pattern is shown on the square grid in Fig. 2. Though a square grid does not allow for as optimal a two-dimensional (2-D) frequency reuse pattern as a hexagonal grid, it is acceptable for the purposes of this study since frequency plans in real systems also often do not follow a standard hexagonal pattern. Macrodiversity (selection of the best available remote antenna by each user) is implemented as follows. By searching over all available pilot signals on all RF frequencies and timeslots, the user could be assigned to any antenna within the downlink square (solid-line type) in Fig. 2. This square includes the antenna(s) nearest to the user at each RF frequency as well as the first-tier antennas at that same frequency (marked with black dots in Fig. 2). These antennas provide the dominant received power contributions at each frequency [13], and in real system operation, the user will be assigned to one of these with very high probability based on which one is detected with the maximum downlink SIR.

Selection diversity is used on both the downlink and uplink in the WACS/PACS system to compensate for near-scale multipath fading. This refers to the use of multiple antennas, separated spatially and/or by polarization at one physical location, to generate uncorrelated near-scale fading channels. The antenna with the highest received SIR at any given time is then selected.

B. Evaluation of Fading and Cochannel Interference

After user placement, the distance loss and both terrain-dependent log-normal fading and multipath Rayleigh fading are computed for the links from the user to each antenna in the downlink square shown in Fig. 2. This is done for both macrodiversity selection and interference computation. The downlink transmit powers of all remote antennas are assumed equal. Since the downlink in WACS/PACS is strongly interference-limited, the thermal noise at the user phone is negligible. Under these conditions, the actual value of the downlink transmit power does not impact the downlink SIR and can thus be normalized to one.

The parameter range used in the simulation for the average distance loss exponent n is 4–6, as described in Section III. The average received power received by user k from remote antenna l in an environment characterized by a specific value of n is known as the global-mean power. The local-mean received power for an individual propagation path is obtained from the global mean by taking into account variations around this mean due to shadowing (8–14 dB, as described in

Section III). This is expressed below:

$$\text{localmean}_{kl}\ (\text{dB}) = 10 \cdot \log_{10}\left(\bar{d_{kl}^{n}}\right) + \sigma N(0,1) \qquad (3)$$

where d_{kl} is the distance from user k to remote antenna l and where $N(0,1)$ is a Gaussian random variable with mean 0 and variance 1.

The terrain-dependent fading is assumed to be uncorrelated for each separate remote antenna. This means that for a given user k, a separate local mean is computed for every remote antenna within its downlink square, as described in Section IV-A. For each of these local means, the Rayleigh multipath fading can be computed as follows:

$$\begin{aligned}\text{amprec}_{klp} &= \text{Rayleigh}_p \cdot \sqrt{10^{\frac{\text{localmean}_{kl}}{10}}} \\ &= \sqrt{(N_i(0,1))^2 + (N_q(0,1))^2}\sqrt{10^{\frac{\text{localmean}_{kl}}{10}}} \qquad (4)\end{aligned}$$

where N_i and N_q are uncorrelated Gaussian random variables with mean 0 and variance 1, and where p is the index of the antenna selected for use through selection diversity. The term *amprec* refers to received signal amplitude at the user antenna. Since selection diversity is used on the downlink in WACS/PACS, two independent Rayleigh samples are generated, corresponding to the different received signal amplitudes at each microdiversity antenna.

The cochannel interference contains contributions from all first-tier (nearest neighbor) remote antennas simultaneously transmitting at the frequency used by remote antenna l. The user selects the remote antenna within the downlink square in Fig. 2 which provides the maximum downlink SIR (each remote antenna uses selection diversity over two microdiversity antennas). This SIR is computed as shown in (5) at the bottom of the page, where the DL square is defined in Fig. 2.

C. Evaluation of Uplink SIR

The uplink SIR for each user is then computed given its selected antenna (which uses frequency 7 for the hypothetical user in Fig. 2). The procedure is very similar to that presented in Section IV-B. Like the downlink, the uplink is also cochannel-interference-limited, so the starting values of all user powers (before power control) are normalized to 1. While the log-normal fading is highly correlated between the uplink and downlink, the Rayleigh fading on the uplink is uncorrelated from that on the downlink due to the 80-MHz separation of the uplink and downlink frequency bands [7]. This results in recomputation of the two Rayleigh values on each uplink. The received uplink SIR at each microdiversity antenna p at a remote antenna l from a given user k can then be expressed as

$$\text{SIR}_{\text{UL}_p}(\text{antenna } l) = \frac{(\text{amprec}_{klp})^2}{\sum_{\substack{i \in \{\text{users in} \\ \text{UL square} \neq k\}}} (\text{amprec}_{ilp})^2} \qquad (6)$$

where the UL square is defined in Fig. 2. (The summation in the denominator is of course over users in a single time slot only.) The microdiversity antenna corresponding to the received RF signal with higher SIR at the base station is selected.

The RF signals sent through fiber from each remote antenna to the base station have the SIR values given in (6). The received signals at the base station have lower SIR values due to further distortion due to fiber-link imperfections. The extent of this degradation is presented in Section V. The RF signal with the larger SIR value at the base station is chosen, and its SIR value is used to determine whether the user power is increased or decreased using power control.

If a user reaches maximum power without reaching adequate SIR performance, then the user is dropped and is counted as not having met the SIR requirement. Since the power control results in all undropped users reaching adequate SIR within 20 or fewer iterations, the aerial availability is simply the percentage of undropped users. We assume that instantaneous fading values can be used to determine the aerial availability, since the 400-Hz power control rate is very fast relative to the temporal multipath fading variations experienced by most users.

V. Analog Optical Links in a PCS Fiber Infrastructure

In this section, the interaction of the WACS/PACS air interface (or wireless link layer) and analog fiber-optic links is described in the context of how the imperfections of analog links will impact PCS quality of service.

A. Block Diagram

For a centralized PCS infrastructure, Fig. 3 shows a block diagram of the analog-link configurations needed on the downlink and uplink for a single connection between a remote antenna and a base station. The configuration shown does not allow sharing of fibers between downlink and uplink or between different remote antennas. (Other infrastructure configurations are considered elsewhere in the literature [3].) On the downlink, a signal modulated on a single RF carrier and composed of several TDMA voice channels (as in WACS/PACS) is amplified and then used to modulate either a laser or an external modulator. This modulated lightwave is transmitted down a fiber to a remote antenna, detected, and subsequently amplified and transmitted from an antenna to its assigned users. The RF carriers drawn with dotted lines

$$\text{SIR}_{\text{DL}}(\text{user } k) = \max_{l \in \{\text{antennas in DL square}\}} \left\{ \max_{p \in \{\text{microdiversity antennas at } k\}} \left[\frac{(\text{amprec}_{klp})^2}{\sum_{i \in \{\text{antennas in DL square} \neq l\}} (\text{amprec}_{kip})^2} \right] \right\} \qquad (5)$$

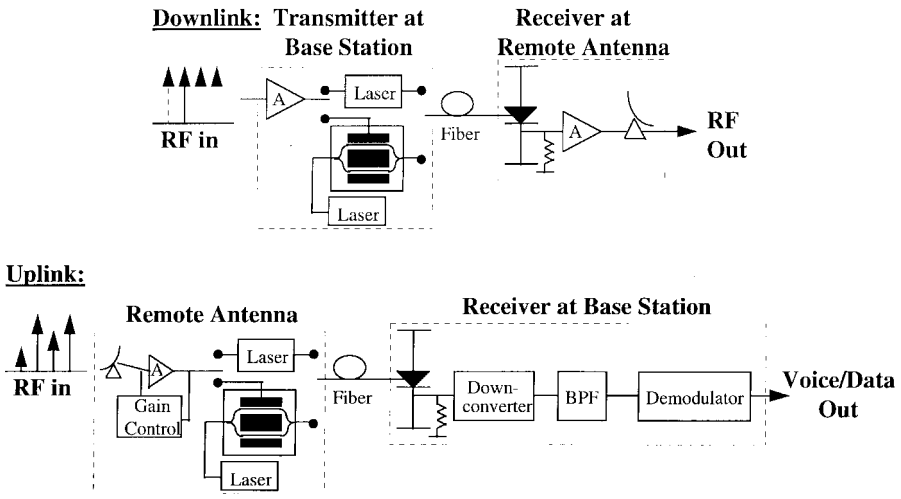

Fig. 3. Block diagrams of analog links on the downlink and uplink in PCS infrastructures.

signify that multiple RF carriers could be used by a single remote antenna.

On the uplink, an RF SCM signal is received at each remote antenna from users simultaneously transmitting on different frequencies. The desired signal from each user is corrupted by both thermal noise from the RF receiver and by cochannel interference. In addition, there are interfering signals on other frequencies due to users transmitting at different RF frequencies. This is known as adjacent-channel interference. (In principle, it is possible to filter out these interfering signals at the remote antenna using a high-Q bandpass filter preceded by a mixer for downconversion. However, this results in more complicated remote antenna units [3].) For example, an antenna receiving a desired uplink transmission on frequency 5 will also receive transmissions on all of the other seven uplink frequencies. Though these interfering signals can be filtered out in the receiver at the base station, third-order nonlinearities due to imperfections in the optical transmitter result in additional nonlinear distortion falling in the desired signal band. The impact of these nonlinearities can become significant if fading conditions are such that the desired signal on the uplink at a remote antenna is much lower than other received signals in adjacent channels.

B. Comparison of Downlink and Uplink

The noise and nonlinearities which degrade the performance of analog fiber-optic links occur on both the downlink and uplink in PCS infrastructures. However, only the degradation on the uplink will have a significant impact on system performance.

On the uplink, the impact of optical-link nonlinearities is far more severe than on the downlink in PCS systems, since the multiple RF carriers transmitted on the uplink have widely varying amplitudes. This is because the propagation paths of different users assigned to a given remote antenna have different propagation distances to the antenna and different shadowing and multipath characteristics. This frequently results in adjacent channel interference (ACI) components that are 30 dB larger than the desired signal, even with power control. (This is because multipath fading in different spatial directions is highly uncorrelated.) In addition, there are many more RF carriers transmitted through the fiber on the uplink (due to users transmitting in adjacent cells) than on the downlink (for which there is only one RF carrier per remote antenna in our model).

Because SIR degradation due to these optical-link imperfections only impacts aerial availability on the uplink, the remainder of this paper focuses on quantifying uplink availability to clarify fiber-link SFDR requirements for infrastructure design.

C. Uplink SIR at the Base Station

The SIR at the input to the demodulator within the base-station receiver in Fig. 3 is shown in (7) at the bottom of the following page, where m is the optical modulation depth and the noise PSD's terms are given in Section II. (R, $P_{\rm opt}$, and b_3 are defined in Section II.) The bandwidth B is 270 kHz, as described in Section III. The noise figure (NF) of the RF amplifiers at the receiver represents the additional thermal noise contribution. Representative parameters for analog links which are used when computing the numerical results in later sections are: responsivity R of 0.8 A/W, a receiver front-end resistance R_r of 50 Ω, an NF of 3 dB, and a semiconductor laser RIN of -150 dB/Hz. $\langle x_i^2(t)\rangle$ refers to the power of the desired signal component at frequency f_i. The value of

$$\frac{\langle x_i^2(t)\rangle}{\langle n^2_{\rm cochannel}(t)\rangle}$$

is defined by the SIR of the received signal from the wireless environment, as shown in (6). The intermodulation power $\langle x^6(t)\rangle$ is the sum of all third-order intermodulation components within $x^3(t)$ which fall into the desired signal band.

The SIR shown in (7) for any given received signal from the wireless environment varies with time due to shadowing and multipath fading. However, the power control rate of 400

Hz used in WACS/PACS is very fast relative to the fading variations experienced by most users. As a result, the fading level remains constant over the period needed by the power control to stabilize. The SIR after power control can then be compared to the desired SIR of 11 dB to determine aerial availability.

D. Dependence of the SIR on SFDR

In the previous section, the modulation depth m, the received optical power P_{opt}, and the third-order nonlinearity coefficient b_3 are not specified. For a given P_{opt} and b_3, there is an optimum modulation depth m which maximizes the SIR in (7). For the simulation results in Section VI, the optimum modulation depth (between 0–1) is found iteratively within the simulation for each separate data point.

To meaningfully determine SFDR requirements for analog links in PCS infrastructures, it is essential that the received SIR at the base station be directly related to the SFDR, since the SFDR is measured using a predetermined two-tone signal. This can be done by solving for b_3 as a function of the SFDR from (1). This gives

$$|b_3| = \frac{8}{3(\text{SFDR})^{3/2}} \frac{R^2 P_{\text{opt}}^2}{2(\text{PSD}_{\text{shot}} + \text{PSD}_{\text{thermal}} + \text{PSD}_{\text{RIN}})B}. \tag{8}$$

As a result, the SIR in (7) can be explicitly written in terms of modulation depth, optical power, and two-tone SFDR. This equation directly relates optical-link quality to received signal quality at the base station, as has been done in previous studies [1].

VI. Simulation Results

The figures in this section show the PCS system availability as a function of optical-link SFDR for representative PCS air interface and analog-link parameters. A power-control range of 30 dB and selection diversity are assumed. The figures show the SFDR requirement for a 0.5% decrease in availability from the perfect fiber case. For very high SFDR optical links, there is an upper limit to availability due to, for example, users that have such a poor uplink propagation environment that the power control range is not sufficient. As the SFDR decreases, the availability decreases due to the increasing SIR degradation due to increasing optical link nonlinearities (thus increasing intermodulation distortion). A system designer could select system SFDR requirements based on a maximum allowable availability decrease due to fiber-link distortion.

Fig. 4 shows the impact of variations in shadowing variance (for example, due to different building or tree heights and densities in different locations) on PCS system performance. A larger shadowing variance results in a lower availability due to an increase in the number of users with very poor propagation environments which cannot be adequately compensated by power control and selection diversity. Also, a larger shadowing variance results in a higher optical-link SFDR requirement (for 0.5% availability decrease). For $\sigma = 8$ dB, the required SFDR is about 76 dB · Hz$^{2/3}$, while for $\sigma = 14$ dB, the required SFDR is about 83 dB · Hz$^{2/3}$. This is because the desired signal will come from one location only, while cochannel and adjacent-channel interference will come from multiple locations. Since the log-normal fading is assumed to be uncorrelated for different locations and directions around a user, the interference will not, on average, increase or decrease for as the value of σ changes. For larger values of σ, the signal received from the worst few percent of environments (for which service may not be available) will decrease relative to the average interference, and thus the SFDR requirement will increase. In reality, there may be some correlation between log-normal fading for interference components from users who are very close to each other. On average though, the impact of SFDR on availability will remain the same.

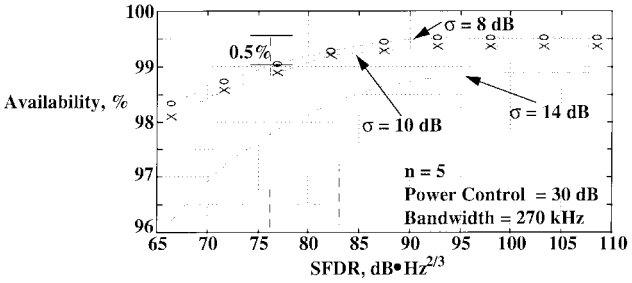

Fig. 4. PCS system availability versus optical link SFDR with selection diversity for shadowing standard deviation $\sigma = 8$, 10, and 14 dB. Dotted lines mark the SFDR for which availability decreases by 0.5%. Distance loss exponent $n = 5$. The power control range is 30 dB.

Fig. 5 shows the impact of variations in distance loss exponent (for example, due to different ground composition or due to variations in environment) on PCS system performance. A larger distance loss results in a higher availability due to the heavily interference-limited characteristic of PCS systems, even for $n = 6$. This, of course, will not be the case indefinitely, since receiver noise and external noise due to the environment will become limiting for large enough n. We also note that a larger distance loss results in a lower optical link SFDR requirement (for 0.5% availability decrease). For $n = 4$, 5, and 6, the required SFDR is about 80, 76, and 72 dB · Hz$^{2/3}$, respectively. This is because the cochannel and adjacent-channel interference almost always are coming from users farther from a given remote antenna than the desired user; as a result, the signal will increase relative to the interference for increasing values of n. This results in less intermodulation distortion due to nonlinearities in the optical link.

$$\text{SIR} = \frac{m^2 R^2 P_{\text{opt}}^2 \langle x_i^2(t) \rangle}{(\text{PSD}_{\text{shot}} + \text{NF} \cdot \text{PSD}_{\text{thermal}} + \text{PSD}_{\text{RIN}})B + m^2 R^2 P_{\text{opt}}^2 \langle n_{\text{cochannel}}^2(t) \rangle + m^6 b_3^2 R^2 P_{\text{opt}}^2 \langle x^6(t) \rangle} \tag{7}$$

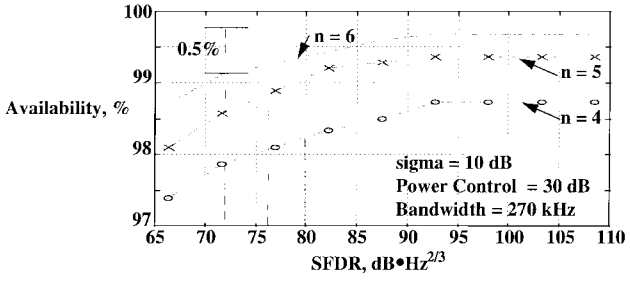

Fig. 5. PCS system availability versus optical-link SFDR with selection diversity for distance loss exponent $n = 4$, 5, and 6. Dotted lines mark the SFDR for which availability decreases by 0.5%. Shadowing standard deviation $\sigma = 10$ dB. The power control range is 30 dB.

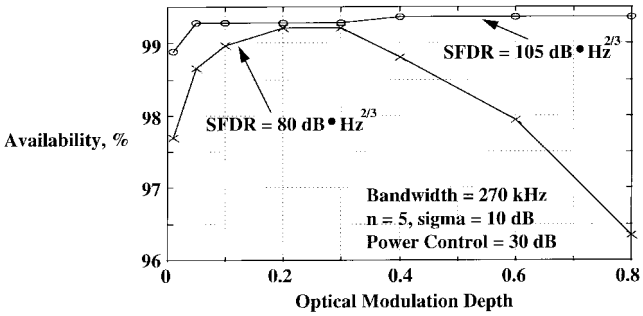

Fig. 6. PCS system availability versus optical modulation depth for two different values of optical link SFDR. The PCS system parameters are shown in the figure.

VII. Discussion

Based on the results of the previous section, it is possible to use either single-mode distributed feedback (DFB) lasers (SFDR range: 90–110 $\text{dB} \cdot \text{Hz}^{2/3}$ [14]) or multimode Fabry–Perot (FP) lasers (SFDR range: 70–90 $\text{dB} \cdot \text{Hz}^{2/3}$ [14]) in PCS systems. This roughly matches the conclusion obtained through modeling of a generic analog cellular system in [1], in which propagation effects within the wireless environment and power control were ignored. A robust design for a PCS fiber infrastructure, however, must be based on an acceptable quality of service over the full range of environments which the system contains. As shown in the previous section, the SFDR requirements can easily vary by almost 10 $\text{dB} \cdot \text{Hz}^{2/3}$ over the range of propagation environments considered in this paper. A system designer using analog optical links as part of a PCS fiber infrastructure should, therefore, augment fiber-link modeling with measured models of the environment to be served when determining fiber-link SFDR requirements.

Another aspect of system design which should be modeled is the sensitivity of system availability to variations of the optical modulation depth from the instantaneous optimal value. Note that the optical modulation depth on the uplink is controlled by an automatic gain control (AGC) loop, as shown in Fig. 3. The goal of the AGC loop is to set the optical modulation depth at a constant value determined by the system designer from timeslot to timeslot. Since it is not possible to dynamically determine the optimum optical modulation depth (which balances the impact of noise and nonlinearities generated in the optical link) for each timeslot at each remote antenna, the system designer can instead use a system-wide constant optical modulation depth which maximizes system availability. Fig. 6 shows the impact of imperfect gain control for a WACS/PACS infrastructure.

It is clear from Fig. 6 that the PCS system availability is more sensitive to optical modulation depth for lower optical-link SFDR. This is because a lower optical-link SFDR corresponds to an optical link with a higher noise level and larger nonlinear distortion. The availability is nearly constant over a 15-dB range of input RF voltage for SFDR $= 105$ $\text{dB} \cdot \text{Hz}^{2/3}$. For an SFDR of 80 $\text{dB} \cdot \text{Hz}^{2/3}$ (within the required SFDR range found in Section VI), availability decreases due to noise for modulation depths which are too low. Also, it decreases due to nonlinear distortion for modulation depths which are too high. To limit the availability decrease (due to nonoptimal optical modulation depth) to 0.5%, the gain control accuracy must be 8 dB.

VIII. Conclusion

Fiber infrastructures in future PCS systems must minimize remote antenna size and cost, reduce the total amount of required RF and digital-processing hardware, and facilitate system maintenance and upgradeability. These goals can be met by a centralized PCS infrastructure using analog fiber-optic links. In this paper, a fiber infrastructure for the WACS/PACS personal communications system has been simulated to evaluate the relationship between optical-link SFDR and wireless system aerial availability.

Results of the simulation indicate that representative SFDR requirements for fiber infrastructures in PCS systems are in the 72–83 $\text{dB} \cdot \text{Hz}^{2/3}$ range. The impact of varying environmental characteristics as quantified by distance loss and shadowing variance is between 7–10 dB. Larger distance loss results in lower SFDR requirements. For example, an increase in the distance loss exponent from 4 to 6 results in a decrease in the SFDR requirement from 80–72 $\text{dB} \cdot \text{Hz}^{2/3}$. Larger shadowing variance results in higher SFDR requirements. For example, an increase in shadowing variance from 8 to 14 dB results in an increase in the SFDR requirement from 76–83 $\text{dB} \cdot \text{Hz}^{2/3}$. The required AGC accuracy decreases as the SFDR increases, with a required accuracy of 8 dB at an SFDR of 80 $\text{dB} \cdot \text{Hz}^{2/3}$. These results indicate that either DFB or FP semiconductor laser diodes can be used in the implementation of PCS infrastructures.

Acknowledgment

The authors would like to gratefully acknowledge helpful discussions with P. B. Wong and X. C. Chen of Stanford University, Stanford, CA.

References

[1] D. M. Cutrer *et al.*, "Dynamic range requirements for optical transmitters in fiber-fed microcellular networks," *IEEE Photon. Technol. Lett.*, vol. 7, pp. 564–566, May 1995.

[2] O. K. Tonguz and H. Jung, "Personal communications access networks using subcarrier multiplexed optical links," *J. Lightwave Technol.*, vol. 14, pp. 1400–1409, June 1996.

[3] W. I. Way, "Optical fiber-based microcellular systems: An overview," *IEICE Trans. Commun.*, vol. E76-B, no. 9, pp. 1091–1102, 1993.

[4] K. Morita and H. Ohtsuka, "The new generation of wireless communications based on fiber-radio technologies," *IEICE Trans. Commun.*, vol. E76-B, no. 9, pp. 1061–1068, 1993.
[5] J. C. Fan, "A fiber infrastructure for microcellular personal communication systems: Infrastructure design and optical dynamic range requirements," Ph.D. dissertation, Dept. Elect. Eng., Stanford Univ., Stanford, CA, 1996.
[6] R. F. Kalman, J. C. Fan, and L. G. Kazovsky, "Dynamic range of coherent analog fiber-optic links," *J. Lightwave Technol.*, vol. 12, pp. 1263–1277, July 1994.
[7] *Generic Criteria for Version 0.1 Wireless Access Communications Systems (WACS)*, Bellcore Standard TR-INS-001313, 1994.
[8] E. A. Lee and D. G. Messerschmitt, *Digital Communication.* Norwell, MA: Kluwer, 1988.
[9] P. B. Wong *et al*., "Low-complexity co-channel interference cancellation and macroscopic diversity for high capacity PCS," in *ICC'95 Proc.*, Seattle, WA, June 1995, pp. 852–857.
[10] D. C. Cox, "Wireless personal communications: What is it?" *IEEE Trans. Prof. Commun.*, vol. 2, pp. 6–21, Feb. 1995.
[11] D. C. Cox, "Universal digital portable radio communications," *Proc. IEEE*, vol. 75, pp. 436-477, Apr. 1987.
[12] H. W. Arnold *et al*., "Macroscopic diversity performance measured in the 800-MHz portable radio communications environment," *IEEE Trans. Antennas Propagat.*, vol. 36, pp. 277–281, Feb. 1988.
[13] R. C. Bernhardt, "Macroscopic diversity in frequency reuse radio systems," *IEEE J. Select Areas Commun.*, vol. SAC-5, pp. 862–870, June 1987.
[14] K. Emura, "Interrelationship of wireless services with optical networks," presented at the *LEOS'95 Conf.*, San Francisco, CA, Oct. 1995.

J. C. Fan, photograph and biography not available at the time of publication.

C. L. Lu, photograph and biography not available at the time of publication.

L. G. Kazovsky (M'80–SM'83–F'91), photograph and biography not available at the time of publication.